Numerical Prediction of Fully Developed Rotating Channel Flow with Functionalized Two-Equation Turbulence Models

S. Dutta and **J.A. Khan**
*Department of Mechanical
Engineering
University of South Carolina
Columbia, SC 29208
USA*

Abstract: Rotating channel flows are important for analyzing the turbine rotor blade internal coolant flow passages where the velocity profile gets skewed by the rotational forces. The velocity increases near the trailing wall and decreases near the leading wall for radial outward flow. Moreover, the turbulent eddy viscosity is higher near the trailing side and low (near laminar) near the leading side. This proximity of high and low turbulence regions are difficult to model by engineering two-equation models and modification of models are required to predict rotational effects. A functionalized C_μ approach is developed for k-ε and k-ω turbulence models that improve prediction of rotating channel flow.

Keywords: *Rotating flow, Turbulence model, Rotor blade coolant passage.*

INTRODUCTION

Several technical papers based on numerical and experimental research are published in the past ten years to analyze the heat transfer in rotating coolant channels simulating the conditions of rotor blade coolant passages. Figure 1 shows the typical cooling arrangement in a turbine rotor blade. There are three regions in a blade that utilizes three different cooling principles. In the leading edge, mostly impingement cooling is used. At the trailing edge, pin fin cooling techniques are employed. In the middle portion, surpentine cooling passages are used. The rotating flow analysis presented here is applicable mostly to the cooling channels in the middle of the blade.

Related important numerical works are: Standard high Reynolds number k-ε model prediction by Prakash and Zerkle [1] and Tekriwal [2]; low Reynolds number k-ε model prediction by Tekriwal [3]; and predictions by Dutta et al. [4,5] on rotating channel heat transfer with an improved rotation induced turbulence production term. This rotation induced turbulence production term was developed by Howard et al. [6]. It is noteworthy that all these numerical predictions are based on two-equation engineering turbulence models. The reason could be, two-equation models are mostly robust and require less computer time to get time averaged turbulence predictions compared to other more detailed turbulence model approaches like, direct numerical simulation (DNS) and large eddy simulation (LES). The computation is inherently three dimensional in rotating channels and hence the required computer time is high and advanced turbulence modeling is not yet cost effective. Figure 2 shows heat transfer predictions by modified k-ε models that compare satisfactorily with experimental results.

The modified model included rotational effects on the turbulence production in the k transport equation. The rotation number, Ro, is the ratio of Coriolis effect to the inertial effect; and

density ratio, DR, represents the effect of rotational buoyancy on the flow. A higher density ratio indicates the effect of buoyancy is stronger on the flow. Since the standard k-ε model is required
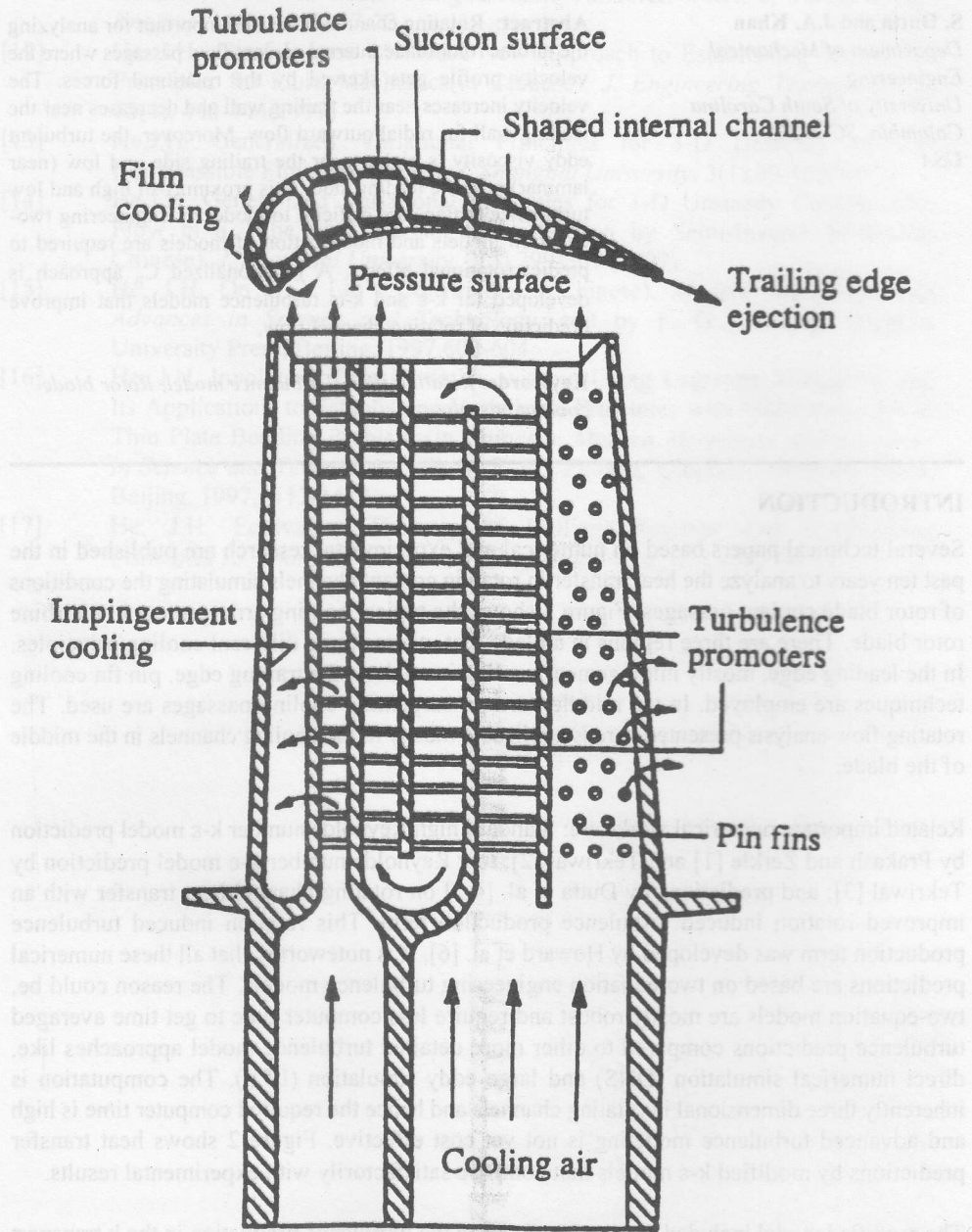

Figure 1: Internal cooling arrangements in a turbine rotor blade (Han et al.[21])

to be modified to correctly predict flows in rotating channels, turbulence models that improve predictions in separated flow conditions are examined here.

This paper compares two different two-equation turbulence model approaches for the prediction of rotating fully developed unheated flows. Note that buoyancy effects may change the flow and turbulence patterns in a heated flow. The selected models have shown improvements in other turbulent flows like, turbulent pipe flows and separated flows [8,14]. The models presented have not been tested before in a rotating field, therefore, the present study provides performance guidance to the numerical researchers about their applicability in rotating channel flow. One of the models used is a two-equation k-ω model of Wilcox [7] to predict rotating channel flow. This method has previously been demonstrated [7,8] to work well in both the fully turbulent and in the transition flow regions. In k-ω model, the wall function approach of high Reynolds number k-ε model is replaced by a calculation up to the boundary walls facilitating more detailed flow analysis in near wall region.

Another model used in this study is the curvature corrected k-ε model of Dutta and Acharya [9]. The curvature-corrected model was developed to predict the separated boundary layer in tripped flow. Since the secondary flow in a rotating channel has significant curvature in the cross-flow plane, curvature corrections on turbulence are applied based on the cross-flow streamline curvature. The turbulence model parameter C_μ is functionalized based on the cross flow velocity gradients and C_μ is varied in the channel cross-section. Predictions by this model reveal a variation of eddy viscosity in the cross flow plane of the rotating channel similar to that observed in experiments.

Our approach of model testing in fully developed rotating turbulent flow is a standard method for model testing in a rotating frame. Other significant research on model testing in rotating channel flow includes Howard et al. [6]. They tested different rotation induced turbulence production terms and their approach was adopted by Dutta et al. [4,5] to predict three-dimensional rotating channel flow and heat transfer with reasonable agreement with experimental heat transfer observation. Pouagare and Lakshminarayana [10] and Galerpin and Kantha [11] developed a rotation corrected C_μ and their expressions for C_μ had a similarity to the Richardson number formulation. We found that it is difficult to achieve good predictions with Richardson number based C_μ and showed that secondary flow curvature-correction approach provides satisfactory convergent results with improvements in the turbulence predictions. Experimental results by Johnston et al. [12] presents a reliable data available in public domain and their work for fully developed two-dimensional rotating flow is used for our performance evaluation.

One important contribution of this paper is the introduction of k-ω model in a rotating frame. The k-ω model is a derivative of the two-equation turbulence model family and has shown improvements in stationary channel flow. Predictions by k-ω model indicate that more research is required to get a satisfactory robust prediction by this model. Discussion on two-equation turbulence models remains incomplete without the mention of the nonlinear k-ε model of Speziale [13]. This two-equation turbulence model simulates the anisotropic behavior of turbulence by nonlinear spatial velocity derivatives and requires computation intensive

filtration techniques. This nonlinear model needs long computer time and may not be of interest for the three dimensional rotating channel flow applications without some modifications to its basic form. Therefore, this model has been excluded from this study and may be tested at a future time.

EXPERIMENTAL CONDITIONS SIMULATED

The experiment of Johnston et al. [12] is taken as the benchmark for this prediction. The channel used for the experiment had a rectangular cross-section, as shown in Figure 3, with a height, h, of 279 mm and width, b, of 39 mm. This high aspect ratio reduced the effects of three-dimensionality in the core flow. The wider sides act as leading and trailing surfaces of rotating channels. The fluid used is water. The inlet velocity for this computational work is selected to be 0.289 m/s corresponding to a Reynolds number of 11,500. Two rotation speeds at 1.553 rad/s and 0.865 rad/s with corresponding rotation numbers of 0.21 and 0.12 are considered. The computation domain extends up to h/2 of the channel to use the symmetry present in the flow.
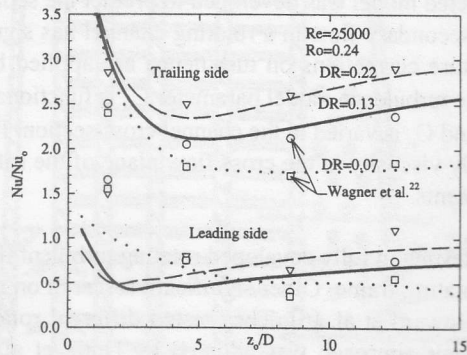
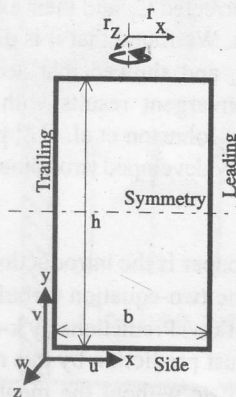Figure 2: Comparison of model predictions with experimental data (Dutta et al.[23])

Figure 3: Channel cross-section and coordinate system

GOVERNING EQUATIONS

This numerical work uses two-equation turbulence models. One of the base models is the standard high Reynolds number k-ε model and the other is k-ω model. The governing equations solved for both turbulence models are:

Continuity equation

$$\nabla \bullet (\rho \overline{V}) = 0 \tag{1}$$

and the solved momentum equations are

$$\nabla \bullet (\rho u \overline{V} - \mu_{eff} \nabla u) = -\frac{\partial \left(p - \dfrac{\rho \Omega^2 r_x^2}{2} \right)}{\partial x} - 2\rho\Omega w$$

$$\nabla \bullet (\rho v \overline{V} - \mu_{eff} \nabla v) = \frac{\partial p}{\partial y} \tag{2}$$

$$\nabla \bullet (\rho w \overline{V} - \mu_{eff} \nabla w) = \frac{\partial \left(p - \dfrac{\rho \Omega^2 r_z^2}{2} \right)}{\partial z} + 2\rho\Omega u$$

where V is the velocity vector (u,v,w). The second term on the right hand sides of the x and z momentum equations, represent Coriolis forces. The centrifugal forces are absorbed in the modified pressures. Centrifugal forces are calculated with rotation radii r_x and r_z in the x and z directions (see Figure 3). The effective viscosity, μ_{eff}, includes laminar viscosity, μ, and turbulent eddy viscosity, μ_t, as

$$\mu_{eff} = \mu + \mu_t \tag{3}$$

STANDARD k-ε MODEL:

The high Reynolds number k-ε model is based on the Boussinesque approximation of the Reynolds turbulent stresses. The eddy viscosity of this model is modeled as

$$\mu_t = \rho \, C_\mu \frac{k^2}{\varepsilon} \; ; C_\mu = 0.09 \tag{4}$$

The k and ε transport equations are

$$\nabla \bullet \left(\rho k \overline{V} - \frac{\mu_t}{\sigma_k} \nabla k \right) = P - \rho\varepsilon \tag{5}$$

$$\nabla \bullet \left(\rho\varepsilon \overline{V} - \frac{\mu_t}{\sigma_\varepsilon} \nabla \varepsilon \right) = C_1 P \frac{\varepsilon}{k} - C_2 \rho \frac{\varepsilon^2}{k} \tag{6}$$

where P is the usual Reynolds stress turbulence production term given as

$$P = \mu_t \left[2\left[\left(\frac{\partial u}{\partial x}\right)^2 + \left(\frac{\partial v}{\partial y}\right)^2 + \left(\frac{\partial w}{\partial z}\right)^2 \right] + \left(\frac{\partial u}{\partial y} + \frac{\partial v}{\partial x}\right)^2 + \left(\frac{\partial u}{\partial z} + \frac{\partial w}{\partial x}\right)^2 + \left(\frac{\partial w}{\partial y} + \frac{\partial v}{\partial z}\right)^2 \right] \tag{7}$$

Due to fully developed flow approximation, $(\partial/\partial z)$ terms are dropped from the governing equations. The $\partial p/\partial z$ is adjusted in the z-momentum equation to achieve the desired flow rate. The near wall region is solved by a wall function.

CURVATURE CORRECTED C_μ

The curvature correction on C_μ can be incorporated by two different coordinate systems. One is based on the stream line (s-n) coordinates and the other is based on Cartesian (x-y) coordinates. The s-n coordinate formulation is more concise and easier to present. Though x-y coordinate formulation derives a long expression for C_μ and looks prohibitive to implement, our experience shows that C_μ based on x-y formulation is numerically well behaved. Acharya et al. [14] showed that x-y coordinate approach had a better agreement with the experimental data compared to s-n coordinate approach for flow past a two-dimensional rib. The final expression for the x-y coordinate was presented in Dutta and Acharya [9] and Acharya et al. [14] but the formal derivation was not included. Therefore, we take the opportunity to present the derivation [15] and related approximations.

The algebraic closure for turbulent stresses [16] can be written as

$$\frac{\overline{u_i' u_j'}}{k} (P - \varepsilon) = P_{ij} + \phi_{ij} - \varepsilon_{ij} \tag{8}$$

where P_{ij} is the production term, φ_{ij} is the pressure strain term and ε_{ij} is the dissipation term. The closure of the pressure strain term is given by Launder et al. [17] as

$$\phi_{ij} = -C_{s1} \frac{\varepsilon}{k} \left(\overline{u_i' u_j'} - \frac{2}{3} \delta_{ij} k \right) - C_{s2} \left(P_{ij} - \frac{2}{3} P \delta_{ij} \right) \tag{9}$$

$$+ C_{s1w} \frac{\varepsilon}{k} \left(\overline{u_i' u_j'} - \frac{2}{3} \delta_{ij} k \right) f\left(\frac{l}{x_w}\right) + C_{s2w} \left(P_{ij} - D_{ij} \right) f\left(\frac{l}{x_w}\right)$$

The term $f(l/x_w)$ represents a near wall function that accounts for near wall viscous damping effects. This term is expressed as

$$f\left(\frac{l}{x_w}\right) = \frac{1}{C_w} \frac{k^{3/2}}{\varepsilon} \left(\frac{1}{x_1^m} + \frac{1}{x_2^m} + \frac{1}{y_1^m} + \frac{1}{y_2^m} \right)^{\frac{l}{m}} \tag{10}$$

where x's and y's are the distance measured from four surrounding walls. The P_{ij} and D_{ij} terms in x-y coordinates can be represented as

$$P_{xy} = -\overline{v'^2}\,\frac{\partial u}{\partial y} - \overline{u'^2}\,\frac{\partial v}{\partial x} \; ; \; D_{xy} = -\overline{u'^2}\,\frac{\partial u}{\partial y} - \overline{v'^2}\,\frac{\partial v}{\partial x}$$

$$P_{xx} = -2\overline{u'^2}\,\frac{\partial u}{\partial x} - 2\overline{u'v'}\,\frac{\partial u}{\partial y} \; ; \; D_{xx} = -2\overline{u'^2}\,\frac{\partial u}{\partial x} - 2\overline{u'v'}\,\frac{\partial v}{\partial x} \qquad (11)$$

$$P_{yy} = -2\overline{v'^2}\,\frac{\partial v}{\partial y} - 2\overline{u'v'}\,\frac{\partial v}{\partial x} \; ; \; D_{yy} = -2\overline{v'^2}\,\frac{\partial v}{\partial y} - 2\overline{u'v'}\,\frac{\partial u}{\partial y}$$

The Reynolds stresses can now be expanded as

$$\frac{\overline{u'^2}}{k} = \frac{\Lambda'}{\varepsilon}\left(-2\overline{u'^2}\,\frac{\partial u}{\partial x} - 2\overline{u'v'}\,\frac{\partial u}{\partial y} - \frac{2}{3}P \right)$$

$$+ \frac{\Lambda''}{\varepsilon}\left(-2\overline{u'^2}\,\frac{\partial u}{\partial x} - 2\overline{u'v'}\,\frac{\partial u}{\partial y} - 2\overline{u'^2}\,\frac{\partial v}{\partial x} - 2\overline{u'v'}\,\frac{\partial v}{\partial x} \right) + \frac{2}{3}$$

$$\frac{\overline{v'^2}}{k} = \frac{\Lambda'}{\varepsilon}\left(-2\overline{v'^2}\,\frac{\partial v}{\partial y} - 2\overline{u'v'}\,\frac{\partial v}{\partial x} - \frac{2}{3}P \right)$$

$$+ \frac{\Lambda''}{\varepsilon}\left(-2\overline{v'^2}\,\frac{\partial v}{\partial y} - 2\overline{u'v'}\,\frac{\partial v}{\partial x} - 2\overline{v'^2}\,\frac{\partial v}{\partial y} - 2\overline{u'v'}\,\frac{\partial u}{\partial y} \right) + \frac{2}{3}$$

$$\frac{\overline{u'v'}}{k} = \frac{\Lambda'}{\varepsilon}\left(-\overline{v'^2}\,\frac{\partial u}{\partial y} - \overline{u'^2}\,\frac{\partial v}{\partial x} \right)$$

$$+ \frac{\Lambda''}{\varepsilon}\left(-\overline{v'^2}\,\frac{\partial u}{\partial y} - \overline{u'^2}\,\frac{\partial v}{\partial x} - \overline{u'^2}\,\frac{\partial u}{\partial y} - \overline{v'^2}\,\frac{\partial v}{\partial x} \right) \qquad (12)$$

where

$$\Lambda' = \frac{1 - C_{s2}}{\dfrac{P}{\varepsilon} - 1 + C_{s1} - C_{s1w}\,f(l/\,x_w)} \; ; \; \Lambda'' = \frac{C_{s2w}\,f(l/\,x_w)\,\Lambda'}{1 - C_{s2}} \qquad (13)$$

Equating the Boussinesq approximation and the algebraic $u'v'$, the following functionalized expression for C_μ is obtained in x-y coordinates, referred to as $C_\mu 1$ and is given by

$$C_\mu 1 = \frac{2/3\ B}{(1 - F - G)(1 - 2kA/\varepsilon)^2}\left(-\Lambda' - 2\Lambda'' + 2A\ \Lambda'\ \frac{k}{\varepsilon}\frac{\left(\frac{\partial v}{\partial x} - \frac{\partial u}{\partial y}\right)}{\left(\frac{\partial u}{\partial y} + \frac{\partial v}{\partial x}\right)}\right) \tag{14}$$

where

$$A = -\Lambda'\frac{\partial v}{\partial y} - 2\Lambda''\frac{\partial v}{\partial y}\ ;\ B = \frac{\Lambda'P}{\varepsilon} - 1\ ;\ F = \frac{k^2\ 2\alpha\beta}{\varepsilon^2\ D}$$

$$\alpha = -\Lambda'\frac{\partial v}{\partial x} - \Lambda''\left(\frac{\partial v}{\partial x} + \frac{\partial u}{\partial y}\right)\ ;\ \beta = -\Lambda'\frac{\partial u}{\partial y} - \Lambda''\left(\frac{\partial v}{\partial x} + \frac{\partial u}{\partial y}\right) \tag{15}$$

$$C = 1 + 2kA/\varepsilon\ ;\ D = 1 - 2kA/\varepsilon$$

This expression of $C_\mu 1$ is solved for each individual computation node and filtered according to a box-filtration technique [18] and then used as local C_μ for turbulent eddy viscosity calculations. Moreover, like other functionalized C_μ models, the range of C_μ is restricted to avoid divergence. The range selected is $0.001 < C_\mu < 1000$, which is a wider range compared to the range $0.025 < C_\mu < 0.2$ adopted by Warfield and Lakshminarayana [19]. Note that this expression for C_μ does not include any rotational terms, however the velocity gradients are affected by rotation and that affects the C_μ value. Pouagare and Lakshminarayana [10] developed a relationship as $C_\mu = 0.09 + \Omega/(\partial w/\partial x)$. We find this approach to be difficult to converge. Any decrease in $\partial w/\partial x$ increases C_μ that in turn increases eddy viscosity. An increase in local effective viscosity decreases the velocity gradient further leading to an unrealistic solution. Therefore, instead of direct summation of stationary and rotational effects, we use a harmonic mean of curvature corrected C_μ and rotation affected C_μ. This approach is similar to the algebraic stress formulation of rotational terms and is given as

$$C_\mu 2 = \frac{1}{\dfrac{1}{C_\mu 1} + \dfrac{\partial w/\partial x}{\Omega}} \tag{16}$$

Model parameter, $C_\mu 2$, calculates the curvature and rotational effects separately and then combines them by a harmonic mean. Note that this formulation may not be suitable for no or low rotation applications because Ω appears in the denominator of Equation (16). Algebraic stress models based on Rodi's [20] approximation are available in the literature and similar functionalized expression for C_μ can be obtained that includes rotational effects.

ROTATION AFFECTED C_μ

The algebraic expression for Reynolds turbulent stress [20] in rotation is

$$\frac{\overline{u'_i u'_j}}{k} = \frac{2}{3}\delta_{ij} + \frac{R_{ij}(2 - C_r 2)/2 + (P_{ij} - 2P\,\delta_{ij}/3)(1 - C_{r2})}{P + \varepsilon(C_{r1} - 1)} \tag{17}$$

where the rotational term is defined as

$$R_{ij} = -2\Omega_p(\varepsilon_{ipk}\overline{u'_j u'_k} + \varepsilon_{jpk}\overline{u'_i u'_k}) \tag{18}$$

We can obtain an expression for C_μ by equating this algebraic stress u'v' to the Boussinesq approximation as

$$C_\mu 3 = \frac{\frac{2}{3}\Omega\varepsilon(2 - C_{r2})(C_{r2} - 1)\partial w/\partial y}{\left(\frac{(P/\rho + \varepsilon(C_{r1} - 1))^2}{k} + \Omega k(2 - C_{r2})(\Omega(2 - C_{r2}) + (C_{r2} - 1)\partial w/\partial x)\right)\left(\frac{\partial u}{\partial y} + \frac{\partial v}{\partial x}\right)} \tag{19}$$

This derived expression is similar to $C_\mu 2$, i.e., the stationary and rotational terms are in harmonic mean and this expression is not recommended for low rotation or stationary channel applications. The $\partial w/\partial y$ in the numerator of Equation (19) makes this $C_\mu 3$ to be high near the side wall and low at the core flow. Computation with this $C_\mu 3$ is hard to converge and no robust converged solution is achieved. However, this expression is retained here for the completeness of the paper.

k-ω MODEL

This is the model proposed by Wilcox [7]. The turbulence transport equations involved are the turbulent kinetic energy, k, and a specific dissipation rate, ω. The dissipation and specific dissipation of k are related as $\varepsilon = \beta^* k\omega$. The eddy viscosity of this model is formulated as

$$\mu_t = \rho\,\alpha^*\,\frac{k}{\omega} \quad or, \quad \mu_t = \rho\,\frac{C_\mu}{\beta^*}\frac{k}{\omega} \quad for\ functional\ ized\ \ C_\mu \tag{20}$$

The k and ω transport equations are

$$\nabla \bullet (\rho k\overline{V} - \frac{\mu_t}{\sigma_k}\nabla k) = P - \rho\,\beta^*\omega k \tag{21}$$

$$\nabla \bullet (\rho\omega\overline{V} - \frac{\mu_t}{\sigma_\omega}\nabla\omega) = \alpha\,P\frac{\omega}{k} - \beta\rho\,\omega^2 \tag{22}$$

where P is the usual Reynolds stress turbulence production term given in Equation (7). The other related terms are

$$\alpha^* = \frac{1/40 + Re_T/6}{1 + Re_T/6} \; ; \; \alpha = \frac{5}{9}\frac{0.1 + Re_T/2.7}{1 + Re_T/2.7}\frac{1}{\alpha^*}$$

(23)

$$\beta^* = 0.09\frac{5/18 + (Re_T/8)^4}{(1 + Re_T/8)^4} \; ; \; \beta = 3/40$$

and the turbulent Reynolds number, Re_T, is defined as

$$Re_T = \frac{\rho k}{\omega \mu}$$

(24)

The near wall boundary implementation technique is described in Wilcox [8]. The constants used in different equations are given in Table 1. A SIMPLER type algorithm solves the pressure and velocity inter-linkages. The flow Reynolds number and wall function requirements in the k-ε model limits the use of fine grids near the wall region. However, non-wall function based k-ω model allows sufficient fine grids for higher resolution near wall. Presented results are with 16x12 grid for wall function based k-ε models and 90x90 for non-wall function based k-ω models. Both two-equation turbulence models have shown satisfactory grid independence.

RESULTS AND DISCUSSION

Figure 4 compares predictions by different functionalized C_μ in k-ε model. Plotted axial velocities and turbulent eddy viscosities are for the symmetry location. The velocity predictions by different functionalization schemes do not show any significant change. Standard k-ε model prediction with $C_\mu=0.09$ is included for comparison. The velocity field is more influenced by the Coriolis term as evident by the near wall increase in the flow for the trailing wall (x/b=0) compared to the leading wall (x/b=1). Curvature correction mostly tends to reduce the core flow and that can be explained from the turbulent eddy viscosity predictions. The experimental velocity measurements are for rotation number 0.21. The increase in axial flow at x/b=0.6 is not satisfactorily captured in predictions. It should be noted that near wall resolution (limited by the wall function) near the leading wall (x/b=1.0) is not sufficient to get detailed flow predictions in that region.

The eddy viscosity predictions show significant difference with different functionalized C_μ expressions. Since the term C_μ has direct influence in the formulation of the eddy viscosity, any change in C_μ changes the eddy viscosity significantly. Though $C_\mu 1$ does not have any formulation based on the rotation speed, eddy viscosity predictions by the $C_\mu 1$ expression shows a peak near the trailing half of the channel. Experimental observation of Johnston et al.[12] for rotation number of 0.12 shows similar turbulent enhancement in the trailing half. A corrective expression based on rotation shows an improvement on the eddy viscosity prediction as shown by predictions with $C_\mu 2$. However, predictions show a smoother eddy viscosity
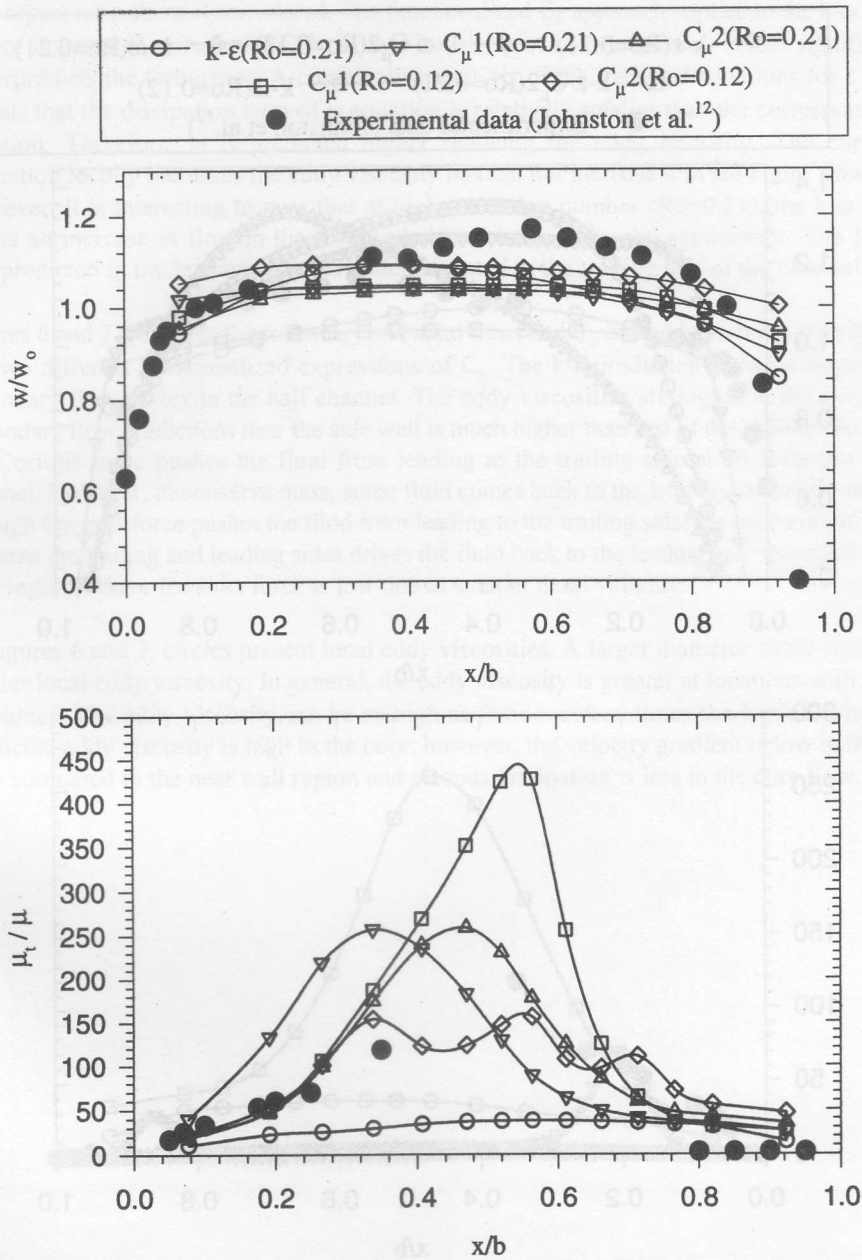
profile by $C_\mu 2$ at higher rotation number.

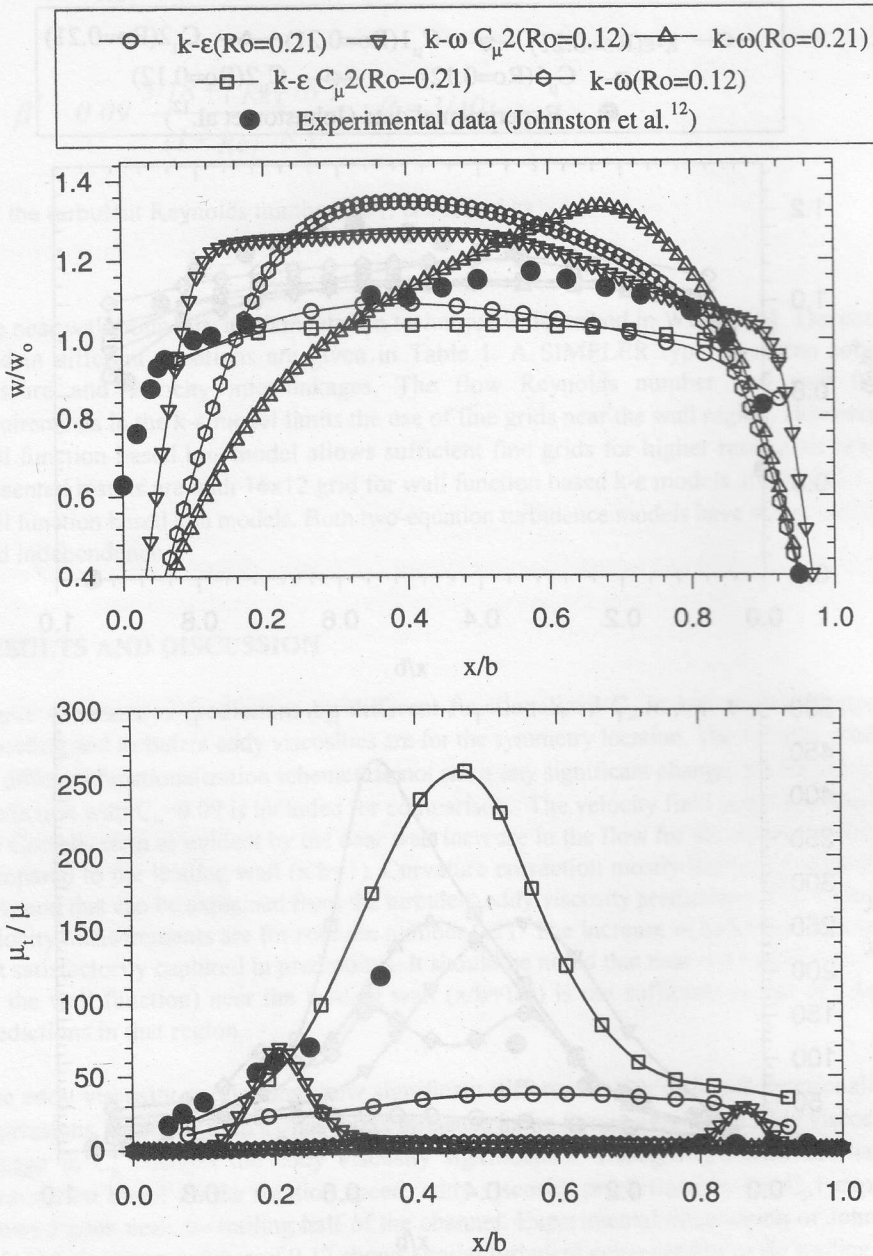

Figure 4: Comparison of predictions by functionalized C_μ

Figure 5: Comparison of predictions by k-ε and in k-ω models

Figure 5 compares the k-ω predictions with the k-ε model. The k-ω model improved predictions in a stationary channel [7] but in rotation predictions are not satisfactory for the high aspect ratio channel considered. The functionalized C_μ approach applied to the k-ω model cannot improve the prediction. The eddy viscosity plot shows that k-ω model significantly underpredicts the turbulence. A comparative analysis of the transport equations for ε and ω reveals that the dissipation term of ω equation is relatively smaller than the corresponding ε equation. Therefore, ω is predicted higher reducing the eddy viscosity. The curvature correction locally increases the eddy viscosity but can not increase it in the entire flow field. However, it is interesting to note that at higher rotation number (Ro=0.21), the k-ω model shows an increase in flow in the leading half as observed by the experiment. The flow is overpredicted in the leading half and underpredicted in the trailing half of the channel.
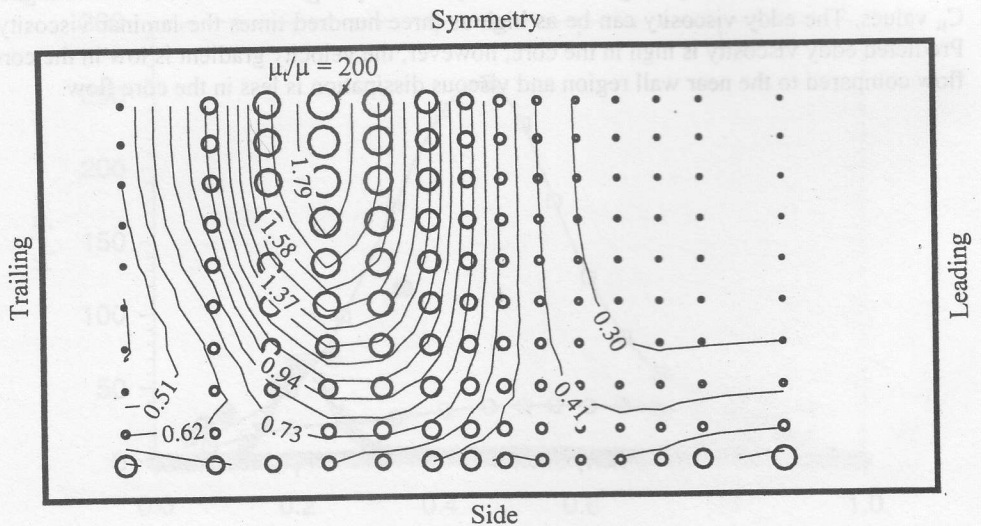
Figures 6 and 7 compares the secondary and axial flow; and C_μ and eddy viscosity distributions for two different functionalized expressions of C_μ. The k-ε prediction shows a single large secondary flow vortex in the half channel. The eddy viscosities are higher at the core flow. Secondary flow predictions near the side wall is much higher than rest of the channel. Note that the Coriolis force pushes the fluid from leading to the trailing side at all locations of the channel. However, to conserve mass, some fluid comes back to the leading half of the channel. Though Coriolis force pushes the fluid from leading to the trailing side, the pressure difference between the trailing and leading sides drives the fluid back to the leading side through the near wall region, where Coriolis force is low due to smaller axial velocity.

In Figures 6 and 7, circles present local eddy viscosities. A larger diameter circle signifies a greater local eddy viscosity. In general, the eddy viscosity is greater at locations with higher C_μ values. The eddy viscosity can be as high as three hundred times the laminar viscosity. Predicted eddy viscosity is high in the core; however, the velocity gradient is low in the core flow compared to the near wall region and viscous dissipation is less in the core flow.
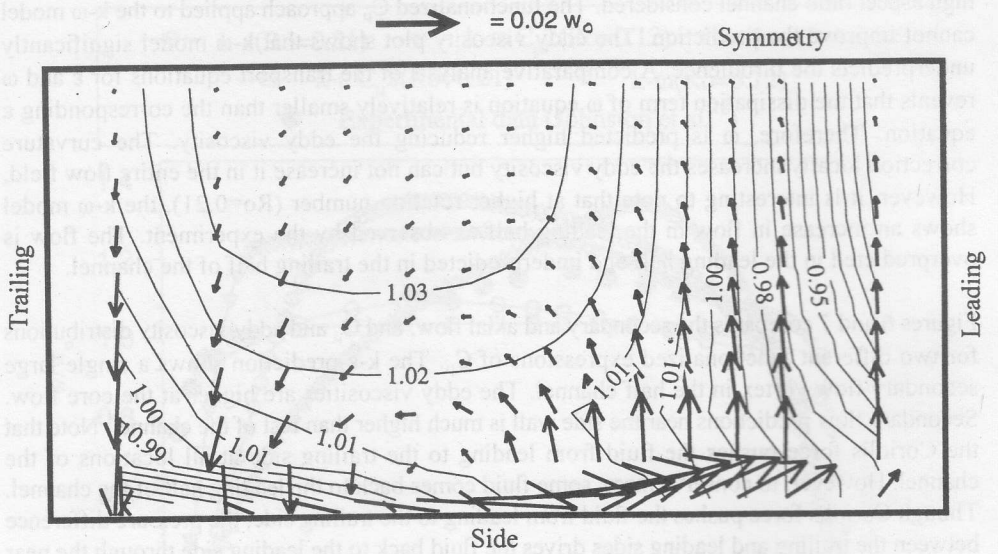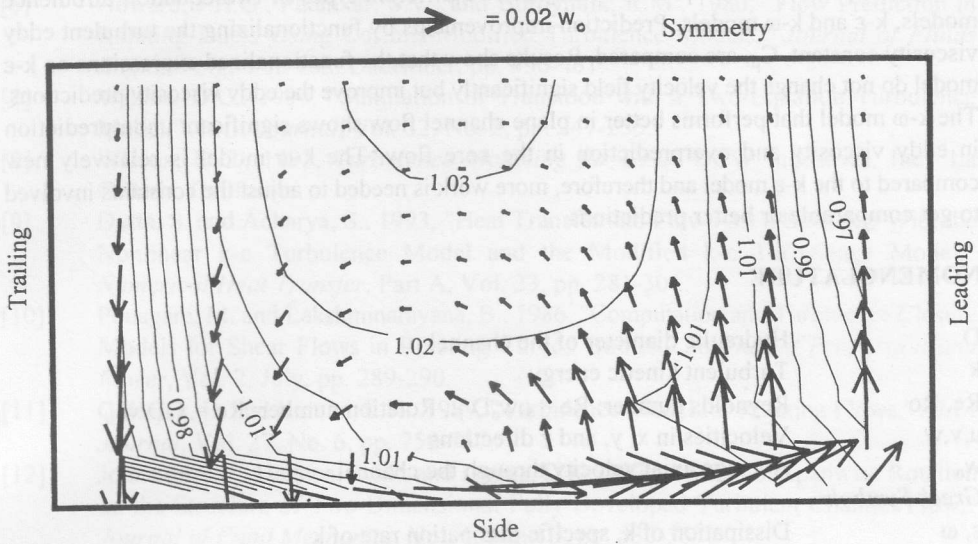
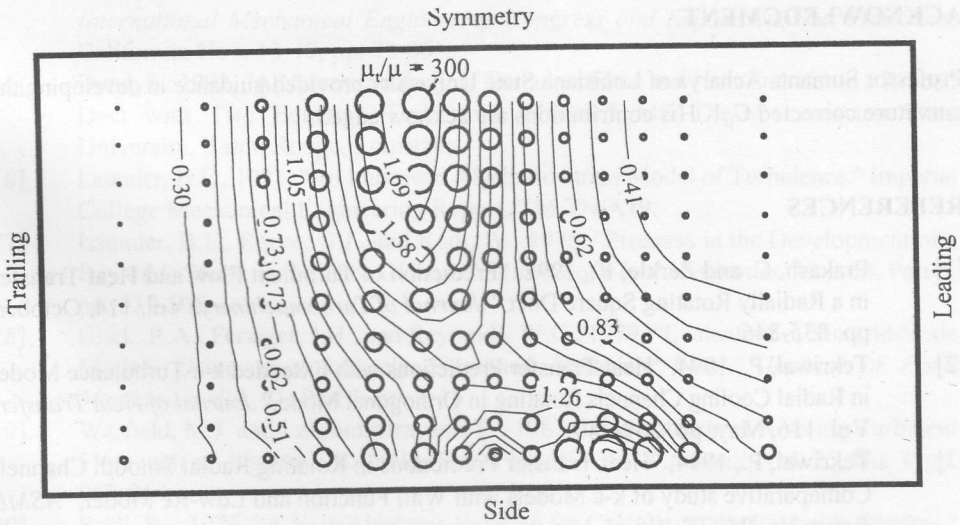(a) Secondary flow vectors and w/w_o contours

(b) $C_\mu 1$ contours and μ_t levels

Figure 6: Predictions by k-ε model and $C_\mu 1$ for $R_o = 0.21$

Symmetry

Trailing

Leading

$\longrightarrow = 0.02\ w_o$

1.03

1.02

0.97

0.99

1.01

1.01

1.01

0.98

1.01

1.01

Side

(a) Secondary flow vectors and w/w_o contours

Symmetry

Trailing

Leading

$\mu_t/\mu = 300$

0.30

1.05

1.69

0.73

0.73

1.58

0.41

0.62

0.62

0.83

0.51

1.26

Side

(b) $C_{\mu}2$ contours and μ_t levels

Figure 7: Predictions by k-ε model and $C_{\mu}2$ for $R_o = 0.21$

CONCLUSION

This paper presents a comparative study of two different types of two-equation turbulence models, k-ε and k-ω models. Prediction improvements by functionalizing the turbulent eddy viscosity constant, C_μ, are compared. Results show that the functionalized expressions on k-ε model do not change the velocity field significantly but improve the eddy viscosity predictions. The k-ω model that performs better in plane channel flow shows significant underprediction in eddy viscosity and overprediction in the core flow. The k-ω model is relatively new compared to the k-ε model and therefore, more work is needed to adjust the constants involved to get comparable or better predictions.

NOMENCLATURE

D	Hydraulic diameter of the channel
k	Turbulent kinetic energy
Re, Ro	Reynolds number: $Re = \rho w_o D / \mu$, Rotation number: $Ro = \Omega D / w_o$
u,v,w	Velocities in x, y, and z directions
w_o	Average axial velocity through the channel
Greek Symbols	
ε, ω	Dissipation of k, specific dissipation rate of k
μ_t, μ	Turbulent and laminar viscosity
Ω, ρ	Rotational speed, density of cooling air

ACKNOWLEDGMENT

REFERENCES

[1]   Prakash, C. and Zerkle, R., 1992, "Prediction of Turbulent Flow and Heat Transfer in a Radially Rotating Square Duct," *Journal of Turbomachinery*, Vol. 114, October, pp. 835-846.

[2]   Tekriwal, P., 1994, "Heat Transfer Predictions with Extended k-ε Turbulence Model in Radial Cooling Channels Rotating in Orthogonal Mode," *Journal of Heat Transfer*, Vol. 116, May, pp. 369-380.

[3]   Tekriwal, P., 1994, "Heat Transfer Predictions in Rotating Radial Smooth Channel: Comaparative study of k-ε Models with Wall Function and Low-Re Model," *ASME Paper No. 94-GT-196.*

[4]   Dutta, S., Andrews, M.J., and Han, J.C., 1996, "Prediction of Turbulent Flow and Heat Transfer in Rotating Square and Rectangular Channels," *ASME Turbo Expo'96*, Birmingham, England, June 10-13.

[5]   Dutta, S., Andrews, M.J., and Han, J.C., 1995, "On the Simulation of Turbulent Heat

Transfer in a Rotating Duct," *AIAA Journal of Thermophysics and Heat Transfer*, Vol. 9, No. 2, April-June, pp. 381-382.

[6]   Howard, J.H.G., Patankar, S.V., and Bordynuik, R.M., 1980, "Flow Prediction in Rotating Ducts Using Coriolis-Modified Turbulence Models," *Journal of Fluids Engineering*, Vol. 102, December, pp. 456-461.

[7]   Wilcox, D.C., 1994, "Simulation of Transition with a Two-Equation Turbulence Model," *AIAA Journal*, Vol. 32, No. 2, pp. 247-255.

[8]   Wilcox, D.C., 1993, *Turbulence Modeling for CFD*, DCW Industries, Inc., La Cañada, California.

[9]   Dutta, S. and Acharya, S., 1993, "Heat Transfer and Flow Past a Backstep With the Nonlinear k-ε Turbulence Model and the Modified k-ε Turbulence Model," *Numerical Heat Transfer*, Part A, Vol. 23, pp. 281-301.

[10]   Pouagare, M. and Lakshminarayana, B., 1986, "Computation and Turbulence Closure Models for Shear Flows in Rotating Curved Bodies," *Journal of Propulsion and Power*, Vol. 2, July, pp. 289-290.

[11]   Galerpin, B. and Kantha, L.H., 1989, "Turbulence Model for Rotating Flows," *AIAA Journal*, Vol. 27, No. 6, pp. 750-757.

[12]   Johnston, J.P., Halleen, R.M., and Lezius, D.K., 1972, "Effect of Spanwise Rotation on the Structure of Two-Dimensional Fully Developed Turbulent Channel Flow," *Journal of Fluid Mechanics*, Vol. 65, Part 3, pp. 533-557.

[13]   Speziale, C.G., 1987, "On Nonlinear k-l and k-ε Models of Turbulence," *Journal of Fluid Mechanics*, Vol. 178, pp. 459-475.

[14]   Acharya, S., Dutta, S., and Myrum, T.A., 1995, "Heat Transfer in Turbulent Flow Past a Surface-Mounted Two-Dimensional Rib," *ASME HTD-Vol. 318, 1995 ASME International Mechanical Engineering Congress and Exposition*, San Francisco, California, Nov. 12-17, pp. 73-86.

[15]   Dutta, S., 1992, "A Numerical Study of Turbulent Flow and Heat Transfer in a Ribbed Duct with Two Equation Turbulence Models," MS Thesis, Louisiana State University, Baton Rouge, Louisiana.

[16]   Launder, B.E., 1971, "An Improved Algebraic Stress Model of Turbulence," Imperial College Mechanical Engineering Report, TM TN/A19.

[17]   Launder, B.E., Reece, G.J., and Rodi, W., 1975, "Progress in the Development of a Reynolds Stress Turbulence Closure," *Journal of Fluid Mechanics*, Vol. 68, Part 3, pp. 537-566.

[18]   Clark, R.A., Ferziger, J.H., and Reynolds, W.C., 1979, "Evaluation of Subgrid-Scale Models Using an Accurately Simulated Turbulent Flow," *Journal of Fluid Mechanics*, Vol. 91, Part 1, pp. 1-16.

[19]   Warfield, M.J. and Lakshminarayana, B., 1987, "Computation of Rotating Turbulent Flow with an Algebraic Reynolds Stress Model," *AIAA Journal*, Vol. 25, No. 7, pp. 957-964.

[20]   Rodi, W., 1976, "A New Algebraic Relation for Calculating the Reynolds Stresses," *Zeitschrift für Angewandte Mathematik und Mechanik*, Vol. 56, pp. 219-221.

[21]   Han, J.C., Chandra, P.R., and Lau, S.C., 1988, "Local Heat/Mass Transfer Distributions Around Sharp 180 Deg Turns in Two-Pass Smooth and Rib-Roughened Channels," *ASME Journal of Heat Transfer*, Vol. 110, pp. 91-98.

[22] Wagner. J.H., Johnson, B.V., and Kooper, F.C., 1991, "Heat Transfer in Rotating Serpentine Passages with Smooth Walls," *ASME Journal of Turbomachinery*, Vol. 114, October, pp. 321-330.

[23] Dutta, S., Andrews, M.J., and Han, J.C., 1996, "Prediction of Turbulent Heat Transfer in Rotating Smooth Square Ducts," *International Journal of Heat and Mass Transfer*, Vol. 39, No. 12, pp. 2505-2514.

Table 1: Values of the constants used for turbulence models

C_1	1.44
C_2	1.92
C_{s1}	1.8
C_{s2}	0.6
C_{s1w}	0.305
C_{s2w}	0.037
C_w	2.44
C_{r1}	1.5
C_{r2}	0.6
m	0.5
σ_k	1
σ_ε	1.3
σ_k^*	2
σ_ω	2